HEALTH AND MEDICINE

Neutrophils preferentially phagocytose elongated particles—An opportunity for selective targeting in acute inflammatory diseases

Hanieh Safari[1], William J. Kelley[1]*, Eiji Saito[2]*, Nicholas Kaczorowski[1], Lauren Carethers[1], Lonnie D. Shea[2], Omolola Eniola-Adefeso[1,2†]

Polymeric particles have recently been used to modulate the behavior of immune cells in the treatment of various inflammatory conditions. However, there is little understanding of how physical particle parameters affect their specific interaction with different leukocyte subtypes. While particle shape is known to be a crucial factor in their phagocytosis by macrophages, where elongated particles are reported to experience reduced uptake, it remains unclear how shape influences phagocytosis by circulating phagocytes, including neutrophils that are the most abundant leukocyte in human blood. In this study, we investigated the phagocytosis of rod-shaped polymeric particles by human neutrophils relative to other leukocytes. In contrast to macrophages and other mononuclear phagocytes, neutrophils were found to exhibit increased internalization of rods in ex vivo and in vivo experimentation. This result suggests that alteration of particle shape can be used to selectively target neutrophils in inflammatory pathologies where these cells play a substantial role.

INTRODUCTION

Neutrophils and monocytes are the most prominent phagocytes in the bloodstream in humans, collectively comprising about 60 to 80% of blood leukocytes (*1*, *2*), because of their essential role as our body's first defense against invading pathogens or responder in the case of injury (*3*, *4*). Furthermore, recent studies have demonstrated that neutrophils are a significant contributor to the in vivo clearance of intravenously injected particles (*5*, *6*). However, neutrophils and monocytes are increasingly negatively implicated in many human pathologies. For instance, neutrophils are vital contributors to the severity of autoimmune diseases, such as antiphospholipid syndrome and multiple sclerosis (*4*, *7*), sepsis (*8*), ischemic stroke (*9*), and chronic inflammatory airway diseases (*10*). Excessive infiltration of neutrophils and increased neutrophilic inflammation (*4*, *10*), or their failure to be recruited to the infection site (*8*), are among the main factors contributing to the severity of these disorders. Alongside neutrophils, inflammatory monocytes also play a significant role in autoimmune disorders, viral infections, and ischemia-reperfusion injury (*11*). Thus, depletion of neutrophils and inflammatory monocytes from the circulation has been investigated for reducing symptoms for the conditions mentioned above (*4*, *10*). Steroids, anti-inflammatory agents, antibodies, and small interfering RNA delivery systems are some of the approaches previously explored for this purpose (*11*, *12*). However, most of these systems either are complex with cytotoxicity issues or have not been fully efficient in delivering a therapeutic benefit (*11*, *13*, *14*).

Recently, researchers have introduced biodegradable particles for targeting blood leukocytes as a strategy for the treatment of or to control the severity of many of the inflammatory conditions mentioned above. As an example, biodegradable particles have been used to modulate immune cells to reduce inflammation and disease symptoms in lupus, spinal cord injury, and sepsis models (*4*, *15*–*17*). However, we know little about the specificity of these systems for targeting various leukocyte subpopulations. Despite their similarities, there have been several reports on structural differences between the different leukocyte subgroups, i.e., neutrophilic polymorphonuclear leukocytes and mononuclear phagocytes (MNPs), which include monocytes, macrophages, and dendritic cells (*18*). The differences in the monocyte chemotactic responses and metabolic burst activity during phagocytosis, their higher level of expression of toll-like receptors, and their capacity for cytokine production compared with neutrophils are among the known differences (*19*). Some recent studies have also reported differences between the interaction of particles with neutrophils compared with other leukocytes. For example, Kelley *et al.* (*20*) recently showed that the presence of poly(ethylene glycol) (PEG) chains on polymeric particle surface increases their phagocytosis by primary human neutrophils, which is the opposite of the observed trend for other phagocytic cells such as macrophages and monocytes.

A compounding factor in our understanding of the interaction of particulate carriers with leukocytes is the fact that most studies have been either in vivo in mice or with immortalized mouse-derived cells in culture, which may not fully capture the behavior of human leukocytes. Furthermore, most of the available literature in this regard have focused on the impact of spherical particle size and surface chemistry on phagocytosis (*21*–*24*). To date, there is a limited understanding of how particle shape prescribes their interactions, i.e., phagocytosis and blood clearance, with circulating leukocytes (*25*) despite a seminal paper by Mitragotri and co-workers (*26*) demonstrating that macrophages do not successfully internalize microparticles from their low curvature side (major axis). A few others validated this finding that sufficiently elongated particles can avoid phagocytosis by macrophages (*27*–*29*), leading to an increase in their in vivo circulation time (*30*). However, considering the differences between the neutrophils and mononuclear phagocytes discussed in the previous paragraph, it remains unclear how neutrophils and other phagocyte groups will internalize particles of varying shapes.

Here, we investigated the effect of particle aspect ratio (AR) on phagocytosis by various human immune cell populations, including

[1]Department of Chemical Engineering, University of Michigan, Ann Arbor, MI 48109, USA. [2]Department of Biomedical Engineering, University of Michigan, Ann Arbor, MI 48109, USA.
*These authors contributed equally to this work.
†Corresponding author. Email: lolaa@umich.edu

neutrophils, monocytes, and macrophages. We demonstrate that the neutrophil response to alterations in the shape of particles is the opposite of the prior observation for mononuclear phagocytes. While rods exhibit reduced phagocytosis by macrophages, monocytes, and dendritic cells, the association of neutrophils with particles significantly increased for rod-shaped particles both in vitro and in vivo. When particles were incubated in whole-blood samples, we found that rods were selectively internalized by neutrophils, with up to sevenfold increased association with neutrophils compared with monocytes. The observed trend of increased phagocytosis of rods by neutrophils was independent of the material type. Our results demonstrate that altering the shape of the micro-/nanoparticles can be used to selectively target the neutrophils for the treatment of the different inflammatory conditions where the neutrophils are the key controllers of the disorder.

RESULTS

Shape dependence of ex vivo uptake of polymeric particles by circulating blood leukocytes

Commercial polystyrene particles of varying diameters (500 nm, 1 μm, and 2 μm) were stretched in a poly(vinyl alcohol) (PVA) film in an oven using a syringe pump as previously described (*31*). The total draw volume of the syringe pump was used to adjust the AR of the particles, and ellipsoidal rods with ARs of 2, 4, and 6 were fabricated, as shown in Fig. 1A. Table S1 shows the sizes of major and minor axes of the particles measured from the scanning electron microscopy (SEM) images, which is in close agreement with the theoretical dimensions of the particles in table S2, i.e., if they were perfect spheroids.

Next, we evaluated the uptake by primary human neutrophils of polystyrene particles of various ARs by incubating fluorescein-labeled particles in whole blood for a 2-hour period. After gating for singlets via flow cytometry, CD45- and CD11b-positive cells were identified, and the neutrophil population was isolated using the forward-scatter and side-scatter panels (fig. S1). The population of the particle-positive cells in the system was quantified by identifying the population of fluorescein isothiocyanate (FITC)–positive cells.

Figure 1B shows the uptake by primary human neutrophils of 2-μm polystyrene spheres and rods of different ARs that were derived from the 2-μm spheres, i.e., having an equivalent spherical diameter (ESD) of 2 μm. Unexpectedly, increasing the AR of these particles increased their association with human neutrophils. However, the difference was only significant for AR6 rods, which had a twofold higher uptake compared with spheres of the same volume. Similar to the 2-μm particles, human neutrophils internalized 1-μm and 500-nm ESD rods more than spheres of the same volume. Moreover, the difference between the internalization of rods and spheres was significant for all the ARs in the 1-μm and 500-nm size range. In particular, the 1-μm AR2 particles exhibited a significant twofold increase in uptake by neutrophils compared with the 1-μm spheres (Fig. 1C). The difference between rods and spheres increased further for the AR4 and AR6 rods having 1-μm ESD, where they respectively had five- and fourfold higher uptake than their spherical counterparts. For 500-nm particles, the concentration of the particles in blood was increased 10 times compared with microparticles to 10^8 particles/ml because of their minimal uptake in the lower concentration range (fig. S2). However, the folds that increase in uptake relative to spheres of the 500-nm ESD rods were smaller compared with the 1 μm for the short rods, with AR2 and AR4 displaying only a 1.5-fold increase in their uptake compared with the spheres. At the largest AR of AR6, the 500-nm rods had a significant fivefold increased uptake relative to their spherical counterparts.

Next, we measured the zeta potential of the spheres and AR6 rods of different sizes to determine whether the increased neutrophil rod uptake is linked to the particle surface charge. As shown in table S3, both the rods and spheres were negatively charged, but with the rods (~−25 mV) being slightly less negative than the spheres (~−40 mV).

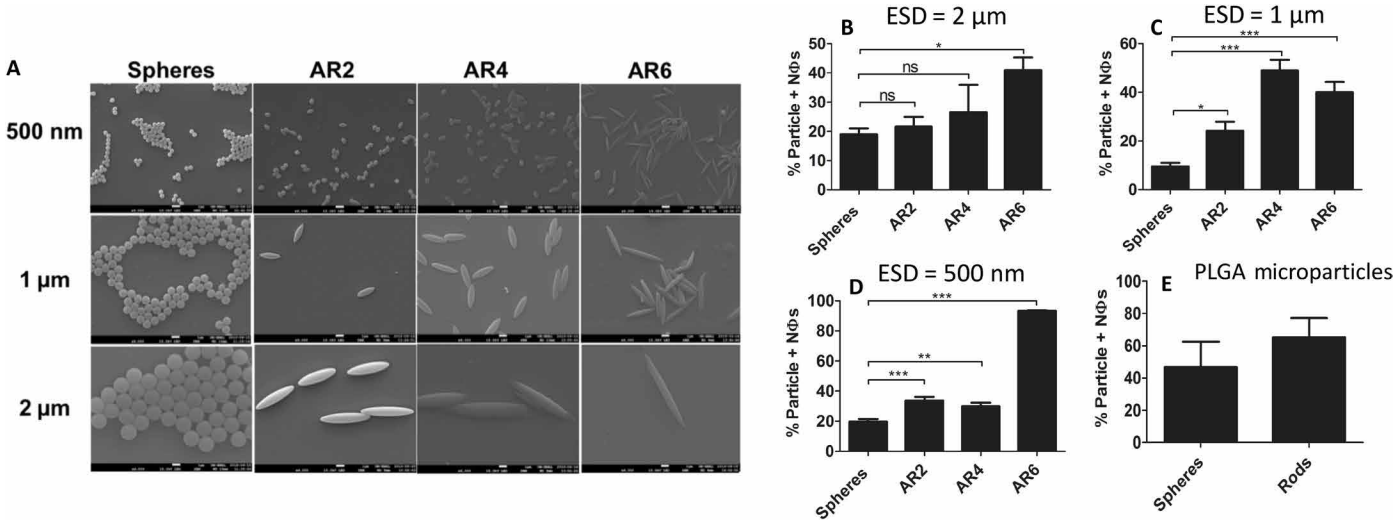

Fig. 1. Ex vivo uptake of particles of different ARs by primary human neutrophils. (**A**) SEM image of the polystyrene particles of different sizes and ARs fabricated via the heat stretching technique in a PVA film. Scale bars, 1 μm. (**B** to **D**) The percentage of primary human neutrophils in whole blood that uptake fluorescent polystyrene particles with equivalent spherical diameters (ESDs) of (B) 2 μm, (C) 1 μm, and (D) 500 nm. The particle concentration in blood was set at 10^7 particles/ml for (B) and (C) and at 10^8 particles/ml for (D). (**E**) Effect of shape on the uptake of poly(lactic-co-glycolic acid) (PLGA) microparticles by primary human neutrophils. The concentration of the particles in blood was set at 5×10^6 particles/ml. One-way analysis of variance (ANOVA) with Tukey's posttest and confidence interval of 95% were used to analyze (B) to (D). Each condition was replicated for at least three individual donors. Unpaired *t* test was used to analyze (E) (ns, $P > 0.05$; *$P < 0.05$; **$P < 0.01$; ***$P < 0.001$).

On the basis of the previous literature, the slightly lower zeta potential value of the rods should lead to decreased phagocytosis if the surface charge is the dominating factor (*32*, *33*), which is the opposite of the trend observed here for their uptake by primary human neutrophils. These zeta potential measurements, thus, confirm that the observed difference in the uptake of rods and spheres by human neutrophils is not a result of the difference in their surface charge.

To see whether the observed increased uptake of rods by neutrophils is valid for other materials, we investigated the uptake of poly(lactic-co-glycolic acid) (PLGA) rods and spheres by primary human neutrophils. Fluorescent (Cy5.5-loaded) spherical and rod-shaped PLGA particles of 1.5 μm ESD were fabricated via a two-step emulsion solvent evaporation technique (fig. S3A), as previously described (*34*). As with polystyrene particles, PLGA rods were taken up by primary human neutrophils at a ~20% higher rate than that of equivalent PLGA spheres (Fig. 1E). However, the differences between rods and spheres were not significant for PLGA particles due to variation in the uptake levels for individual donors and, likely, the heterogeneity in the PLGA particle size within a given sample. Nevertheless, rods were consistently internalized more than spheres for each donor (fig. S3B).

Next, we examined the uptake of the particles of different shapes by monocytes and monocyte-derived cell lines. First, we evaluated isolated primary human monocytes in plasma. Isolated monocytes were used in this study because of the low population of the human monocytes in whole blood compared with neutrophils and lack of a specific monocyte marker. As represented in Fig. 2A, the isolated human monocytes' uptake of rods was not significantly different from that of spheres. Conversely, for assays with cultured Tamm-Horsfall Protein 1 (THP-1) monocytes, we find rods exhibited five- and sixfold lower uptake than the spherical particles of the same volume for the ESDs of 500 nm and 1 μm, respectively, which is the opposite of the trend observed for neutrophils (Fig. 2B).

To determine whether the observed trend for human neutrophils is species dependent, we investigated the uptake of AR6 rods and spheres of different sizes by normal and inflamed mouse blood. AR6 rods were used in these experiments because of their consistently higher uptake by primary human neutrophils compared with the spheres across all the size ranges (Fig. 1, B to D). Neutrophils in mouse blood were identified by gating out CD45-, CD11b-, and Ly6G-positive cells. Particle-positive cells were quantified by gating the population of the FITC-positive cells (fig. S4). Figure 3 shows that, independent of the mouse strains evaluated, rods of all different sizes had a significantly higher uptake by neutrophils compared with spheres. In the BALB/c mouse blood, 500-nm, 1-μm, and 2-μm AR6 rods had an approximately 1.5-fold higher uptake than spheres (Fig. 3A). We observed the same trend for the experimental autoimmune encephalomyelitis (EAE) model of the SJL/J mouse strain. Because of the saturation of the EAE mice neutrophils by 2-μm particles at the 2-hour uptake point (fig. S5), we opted to investigate the uptake at the 30-min time point. At the 30-min time point, EAE neutrophils in blood internalized rods with ESDs of 500 nm, 1 μm, and 2 μm at 7-, 7.5-, and 4-fold higher than the spheres of the same volume, respectively, which was consistent with the trend observed for the BALB/c mice and human neutrophils (Fig. 3B). Again, in contrast to neutrophils, BALB/c mouse monocytes phagocytosed rods at the same or lower level than the spheres of the same volume (Fig. 3A). When we compare the uptake of the particles by neutrophils and monocytes for BALB/c mice, we find that rods had 2.5-, 4.5-, and 7-fold higher association with neutrophils compared with monocytes for the 500-nm, 1-μm, and 2-μm particles, respectively. In the EAE model, monocytes internalized rods higher than the spheres, similar to neutrophils (Fig. 3B). However, a head-to-head comparison between EAE mouse neutrophils and monocytes shows that neutrophils internalized rods by ~3.5-fold more than monocytes for the 500-nm and 1-μm particles. For the 2-μm particles in EAE mouse blood, however, rods were internalized at the same level by both monocytes and neutrophils. These results demonstrate that the rod shape, coupled with size, can be used to target neutrophils in circulation selectively while keeping the respective uptake by monocytes minimum.

Shape dependence of uptake of polymeric particles by blood leukocytes in vivo

To confirm that the observed in vitro trends described above exist in vivo, we investigated the uptake of particles by leukocytes in BALB/c mice injected with either 500-nm polystyrene spheres or AR6 rods in vivo. We chose 500-nm particles and AR6 rods for in vivo assays because of the maximum difference between the association of rods and spheres with neutrophils that was observed for this size with in vitro assays, as represented in Fig. 1D. In addition, there is more interest in the use of smaller-sized particles in clinical trials because of the lower risk of inducing occlusion in smaller capillaries. After particle injections, blood was drawn from the animals

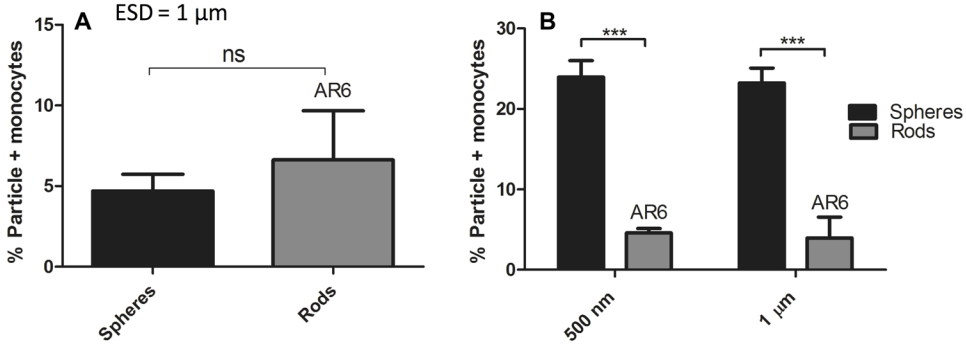

Fig. 2. Shape dependence of phagocytosis by human monocytes. Uptake by (**A**) isolated human monocytes in plasma ($n = 3$ individual donors for each condition) of polystyrene spheres or AR6 rods with an ESD of 1 μm and (**B**) THP-1 monocytes in RPMI media of polystyrene spheres and AR6 rods with ESDs of 500 nm and 1 μm. The concentration of the cells and particles was set at 10^6 cells/ml and 10^7 particles/ml, respectively. An unpaired *t* test was used to analyze (A) and two-way ANOVA with Bonferroni posttest for (B) (ns, $P > 0.05$; ***$P < 0.001$).

via cardiac puncture 30 min after injection, and the association of the particles with monocytes and neutrophils was evaluated via flow cytometry. The in vivo results confirmed the observed ex vivo trend. While there was not a significant difference between the uptake of the rods and spheres by monocytes, mouse neutrophils in vivo preferentially phagocytosed rods compared with the spheres. Specifically, rods had threefold higher uptake than the spheres of the same volume by mouse neutrophils in vivo (Fig. 4).

While a few studies have evaluated the circulation time and tissue distribution of prolate rods in vivo in mice, none have done so in parallel with the analysis of phagocytosis by blood leukocytes. Thus, we analyzed the tissue distribution of the 500-nm spheres and AR6 rods at the 30-min postinjection time used for the in vivo uptake studies. The results show a preferential accumulation of spheres in the liver, while more rods were found in the spleen and lungs (fig. S6). This particle tissue distribution pattern is consistent with the previous studies where the increase in AR for nanoparticles was shown to decrease their accumulation in the liver while increasing it in the lungs and spleen for shorter time points (*35*, *36*). Furthermore, the lower accumulation of the rods in the liver and, thus, their increased accumulation in other organs can be attributed to their lower uptake by liver macrophages (*27*).

Competitive uptake of rods and spheres by neutrophils

Competitive uptake assays conducted with 2-μm rods and spheres also confirmed the preferential uptake of rods by human and mouse neutrophils, i.e., spheres and rods, each with a different fluorescent label, were simultaneously present in the sample at the same concentration. The AR6 rods were associated with human neutrophils about threefold higher than the spheres of the same volume despite both particle shapes being simultaneously available for cell eating (Fig. 5A). Further analysis revealed that less than 10% of the human neutrophils internalize only spheres, while approximately 35% of them were associated with rods only. About 15% of the human neutrophils internalized both rods and spheres simultaneously (Fig. 5B). The same trend was observed for mouse neutrophils, where there were around 3.5-fold higher number of the neutrophils associated with the rods compared with the spheres (Fig. 5C). In addition, only about 5% of the mouse neutrophils internalized only spheres, while ~55% of the cells only phagocytosed rods. About 15% of mouse neutrophils internalized both the rods and spheres (Fig. 5D).

The increased association of the neutrophils with the rods in the competitive uptake assays was also confirmed via microscopy. As shown in Fig. 5E, a higher number of rods were colocalized with the human neutrophils compared with spheres. Quantification of the

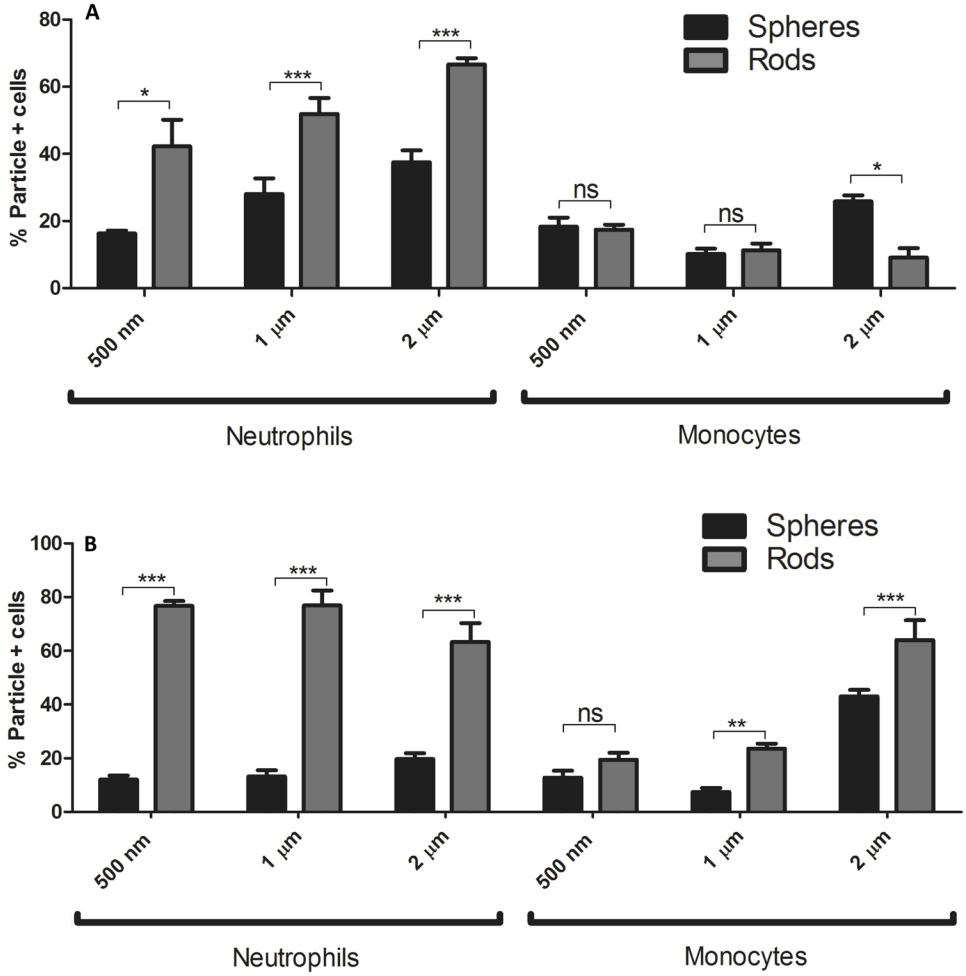

Fig. 3. Ex vivo uptake of rods and spheres in whole mouse blood. Uptake of polystyrene spheres and AR6 rods of different sizes by mouse neutrophils and monocytes in blood obtained from (**A**) 6- to 8-week-old male BALB/c and (**B**) 9- to 11-week-old female experimental autoimmune encephalomyelitis (EAE) model of SJL/J. The concentration of the particles in blood was set at 10^7 particles/ml. Two-way ANOVA with Bonferroni posttest was used for analyzing the data (ns, $P > 0.05$; *$P < 0.05$; **$P < 0.01$; ***$P < 0.001$).

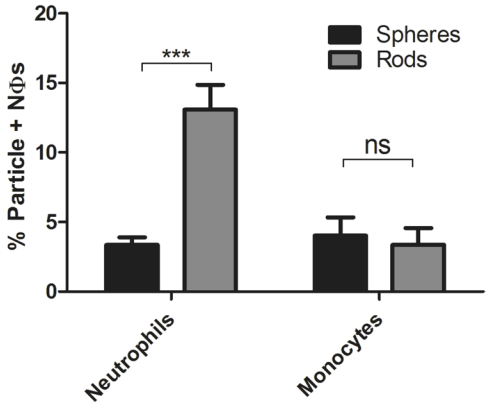

Fig. 4. In vivo uptake of the 500nm polystyrene spheres and AR6 rods of the same volume by mouse neutrophils and monocytes. Particles (5×10^9) (either rods or spheres) were injected into each animal, and the blood was drawn from the animals 30 min after injection. Healthy 6- to 8-week-old male BLAB/c mice were used for the in vivo experiments. Two-way ANOVA with Bonferroni posttest was used for analyzing the data (ns, $P > 0.05$; ***$P < 0.001$).

number of particles associated with cells in multiple images showed that about 85% of spheres were free in the mixture without being internalized by any cells. This number decreased to 60% for the rods, which confirms the preferential association of the rods with neutrophils. To summarize, the results here demonstrate that the preference of neutrophils for internalizing rods remains valid even with both the rods and the spheres present in the same sample.

Preferential uptake of rods is unique to neutrophils

The results presented in previous sections demonstrating the preferential uptake of rods by blood neutrophils are unexpected and counter the general understanding to date of the impact of shape on particle phagocytosis and blood circulation in vivo. Several published studies have demonstrated that rods are phagocytosed by macrophages significantly less than their spherical counterparts (*26*), and these observations were often projected to all leukocytes. To confirm the unique observation that neutrophil's preference for rods is not an artifact of our system, we investigated the uptake of particles of different shapes by the cells evaluated in prior publications, i.e., mouse and rat macrophages and dendritic cells.

Similar to prior publications, bone marrow–derived macrophages evaluated in our system preferentially phagocytosed spheres. Spheres were taken up six- and fivefold higher than AR6 rods of the same volume, respectively, for particles with ESDs of 500 nm and 1 μm (Fig. 6A). Similarly, rat alveolar macrophages also exhibited three- and fivefold higher uptake of spheres than AR6 rods for particles with ESDs of 500 nm and 1 μm, respectively (Fig. 6B). Because of the minimal uptake of the 500-nm particles by the rat alveolar macrophages when at the same concentration as microparticles, the uptake was not significantly different between rods and spheres for this size. When the concentration of the 500-nm particles was increased to 10^8 particles/ml and the concentration of the cells lowered to 10^6 cells/ml, the difference between the rods and spheres became significant for the 500-nm particles as well. Spheres of this nanometer size had 16-fold higher uptake by alveolar macrophages than the rods of the same volume (fig. S7). Our results demonstrated that macrophages followed the same general observed trend of the preferential uptake of the spheres reported in previous works, showing that phagocytosis of microparticles by macrophages can be inhibited by using elongated particles.

The same trend of inhibited phagocytosis of rods was also observed for dendritic cells. When the concentration of the particles was fixed at 10^7 particles/ml, which is two times higher than the cell concentration, 500-nm and 1-μm spheres had 2.5- and 4-fold higher uptake than the rods of the same volume, respectively (Fig. 6C), but the difference was not significant for the 500-nm ESD. At the higher concentration of 10^8 particles/ml, the difference between the uptake of the 500-nm rods and spheres was shown to be significant, with spheres exhibiting sevenfold higher uptake than the rods of the same volume (Fig. 6D). To summarize, our results in this section show that both macrophages and dendritic cells favorably phagocytosed spheres compared with the high AR particles, following the same trend as monocytes.

DISCUSSION

Our results here have demonstrated that, contrary to the trend observed for mononuclear phagocytes, neutrophils preferentially phagocytose rod-shaped particles. Increasing the AR of the particles increases their association with and uptake by human and mouse neutrophils. The observed trend remains valid when the competitive uptake of the rods and spheres was investigated as well, where neutrophils were favorably associated with the rods compared with the spheres. In whole-blood samples, when both the neutrophils and monocytes were present, the neutrophils significantly favored the rods compared with monocytes.

The previously reported reduced internalization of the ellipsoidal particles by macrophages was attributed to the energy requirement for actin remodeling necessary for engulfment of the high AR particles (*28*). Previous studies reported rods to have increased attachment to macrophages, but the energy required for the actin remodeling limits their internalization and phagocytosis rate (*28*). The observed differences between the response of the neutrophils and MNP phagocyte groups might be attributed to the differences in their phagocytic mechanisms. Neutrophils generally have higher mobility than the other phagocytes, including both monocytes and macrophages (*18*). It has also been shown that when engulfing untargeted microparticles, the cellular pedestal of the neutrophils goes through protrusion in the direction of the target in the initial phases of phagocytosis, which shows their capability for remodeling their actin network during phagocytosis (*37*, *38*). The amount of cortical tension and viscosity is an order of magnitude higher for macrophages compared with neutrophils. All these mentioned studies imply higher stiffness and lower surface motility for macrophages compared with neutrophils (*39*). Furthermore, in contrast to macrophages, phosphorylation of the fragment crystallizable gamma receptor (FcγR) receptors is not essential for the phagocytic activity of neutrophils (*40*). Thus, the increased motility of the neutrophils compared with MNP phagocytes and the nonnecessity of phosphorylation during phagocytosis likely translate to their lower energy barrier for actin remodeling and engulfment of the elongated particles compared with the other phagocyte groups.

Furthermore, phagocytosis is a two-step process consisting of the attachment and internalization of the particles (*24*). The lower energy barrier for the actin remodeling can change the rate-limiting step in the phagocytosis process for the neutrophils. Once this energy barrier for the actin remodeling is overcome, the extent of the phagocytosis can be a consequence of the interplay between the attachment rate,

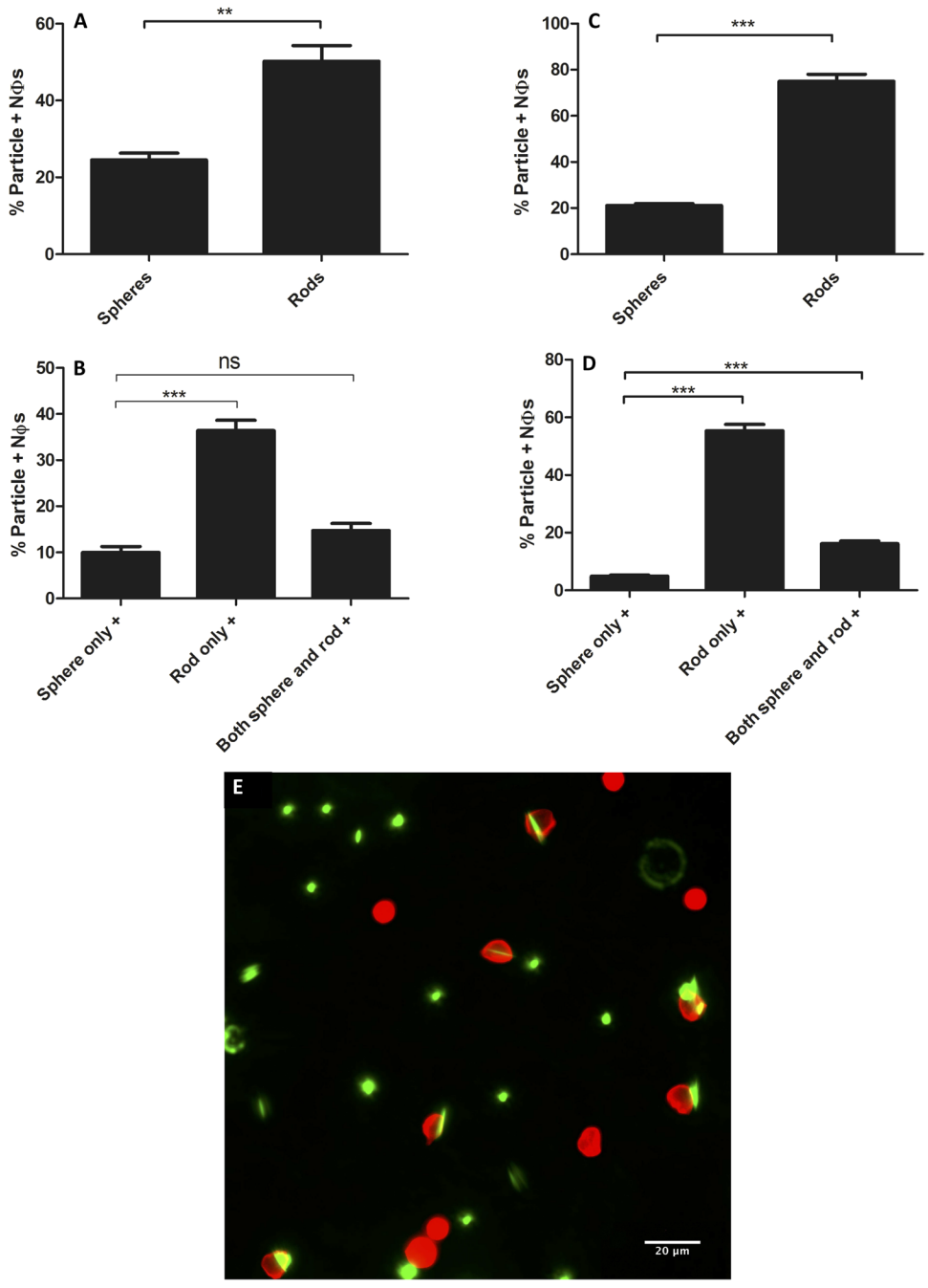

Fig. 5. Competitive uptake of 2µm spheres and AR6 rods by primary human and mouse neutrophils. The total population of the human neutrophils that were (**A**) rod positive or sphere positive and (**B**) internalized only rods, spheres, or both rods and spheres. The total population of the mouse neutrophils that were (**C**) rod positive or sphere positive or (**D**) internalized only rods, spheres, or both the rods and the spheres. (**E**) Fluorescence image representing the competitive uptake of the rods and spheres by human neutrophils. The cells are red, and the particles are green. Two-micrometer spheres and AR6 rods of the same volume were used in all experiments represented in the figures. One-way ANOVA with Tukey's posttest was used to analyze (B) and (D), and unpaired *t* test was used to analyze (A) and (C) (ns, $P > 0.05$; $^{**}P < 0.01$; $^{***}P < 0.001$).

particle volume, and major axis size. As our results show, for the size range studied in our work, increasing the size of the particles increases their uptake by neutrophils for the matched concentration of the particles in the blood, which is in line with the results of the previous studies that have investigated the impact of size on phagocytosis of the particles by primary human neutrophils (*20*, *23*). The previously reported higher attachment of the rods to the phagocytes (*28*) and the increase in the major axis length by increasing the AR of the particles may then explain the observed higher internalization of the particles by neutrophils. However, the major axis length is not the sole determining factor of the phagocytosis by neutrophils. The AR6 500-nm rods and AR2 1-µm rods both have the same major

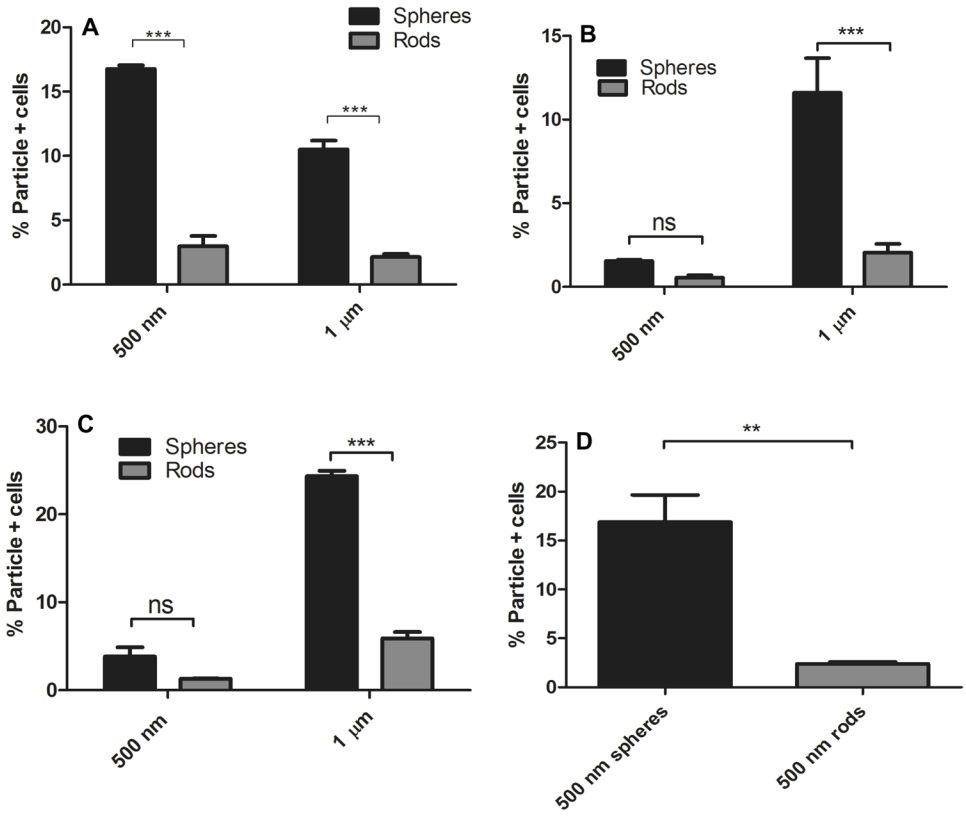

Fig. 6. The shape dependence of the phagocytosis of polymeric particles by macrophages and dendritic cells. Uptake of the spherical and AR6 rod-shaped polystyrene particles of different sizes by (**A**) mouse bone marrow–derived macrophages and (**B**) rat alveolar macrophages in RPMI media. The concentration of the particles was fixed at 10^7 particles/ml, and the concentration of the cells was set at 5×10^6 and 10^7 cells/ml, respectively, for mouse bone marrow–derived and rat alveolar macrophages. Uptake of rods and spheres of different sizes by mouse bone marrow–derived dendritic cells with the fixed particle concentration of (**C**) 10^7 particles/ml and (**D**) 10^8 particles/ml. The concentration of the cells was fixed at 5×10^6 cells/ml. Two-way ANOVA with Bonferroni posttest was used for analyzing (A) to (C), and unpaired *t* test was used for analyzing (D) (ns, $P > 0.05$; $^{**}P < 0.01$; $^{***}P < 0.001$).

axis length, but the uptake of the 500-nm rods (fig. S2) is significantly lower than that of the 1-μm rods (Fig. 1C) for the matched concentration, possibly due to their smaller volume.

As discussed previously, targeting the neutrophils in different inflammatory conditions is a potential strategy for controlling the disease and its progression (*4*, *15*, *16*). The results of this study show the specificity of rods to neutrophils, even in inflammatory conditions like EAE, for particle sizes of 1 μm or smaller. Previous works have also demonstrated that optimization of the particle design parameters, like hydrophobicity, to maximize their association with the neutrophils will increase their therapeutic benefit as inflammation modulators (*4*, *16*). We posit that this observed desirability of the rods to get associated by neutrophils can be used to specifically target neutrophils in disease models where neutrophils are the key player while benefiting from their reported prolonged circulation times and minimum uptake by other phagocytes to increase their therapeutic efficacy.

In conclusion, our work has investigated the response of neutrophils to variations in particle shape. This feature can be used to target neutrophils to reduce their trafficking to inflammation sites or to deliver a specific drug to these cells. In future work, rod-shaped particles could be used in various disease models where neutrophils are the key targets to see whether the use of the elongated particles, which benefit from increased association with neutrophils, can help to improve the treatment status of these conditions. The future use of such particle shape–based targeting to neutrophils will require researchers to have easy access to biocompatible and biodegradable, nonspherical particles, such as the PLGA spheroids used here. Naturally occurring, rod-shaped particles like halloysite nanotubes can also be used in this regard (*41*).

MATERIALS AND METHODS

Experimental design

Our experiments were designed to investigate the effect of AR on the association of the polymeric particles with different phagocyte groups. Particles of different ARs were fabricated, and their association with neutrophils, monocytes, macrophages, and dendritic cells were quantified and compared to each other. The comparative uptake of the particles of different shapes in whole-blood samples was evaluated both ex vivo and in vivo. We compared the shape dependence of the uptake for neutrophils and mononuclear phagocytes. All the human donors for the experiments were healthy. The animal blood was collected from both healthy and EAE model mice. In vivo experiments were performed on healthy mice. All the experiments were replicated at least three times.

Study approvals

Human blood from healthy donors was obtained via venipuncture per a protocol approved by the University of Michigan Internal Review

Board. A written consent was obtained from the individuals before the blood draw.

Animal studies were conducted in accordance with National Institutes of Health *Guidelines for the Care and Use of Laboratory Animals* and approved by the Institutional Animal Care and Use Committee of the University of Michigan. All mice were housed under specific pathogen–free conditions and maintained in the University of Michigan in compliance with the University Committee on Use and Care of Animal regulations.

Materials

Poly(DL-lactide-co-glycolide) (50:50) (inherent viscosity = 0.66 dl/g) with carboxylic acid end groups were purchased from DURECT Corporation (Cupertino, CA). Proteolipid protein (HSLGKWLGHPDKF) (PLP139-151) was purchased from GenScript USA Inc. (Piscataway, NJ). Cyanine 5.5 (Cy5.5) amine dye was purchased from Lumiprobe (Florida, USA). Dichloromethane (DCM), chloroform, *N*-(3-dimethylaminopropyl)-*N*′-ethylcarbodiimide hydrochloride (EDC), PVA, 2-mercaptoethanol, and Trizma base were purchased from Sigma-Aldrich (St. Louis, MO). *N*-hydro-xysuccinimide (NHS) was purchased from Thermo Fisher Scientific (Waltham, MA). Fluoresbrite YG carboxylate microspheres of different sizes were purchased from Polysciences (Warrington, PA). Two-micrometer sky blue polystyrene carboxylate microspheres were purchased from Spherotech (Lake Forest, IL). Granulocyte-macrophage colony-stimulating factor (GM-CSF) was purchased from PeproTech (Rocky Hill, NJ). Human monocyte isolation kit was purchased from BioVision Incorporated (Milpitas, CA). Cell Dissociation Buffer Enzyme-Free Hanks'-Based was purchased from Life Technologies (Carlsbad, CA). *Mycobacterium tuberculosis* H37Ra was purchased from Difco (Detroit, MI). Sodium metaphosphate (SMP) was purchased from Alfa Aesar (Haverhill, MA). Fetal bovine serum (FBS) was purchased from Atlanta Biologicals (Flowery Branch, GA). Anti-human CD45, anti-mouse/human CD11b, anti-mouse CD45, anti-mouse Ly-6G, and anti-mouse Ly-6C antibodies were purchased from BioLegend (San Diego, CA).

Fabrication of polystyrene rods

Polystyrene carboxylated microspheres were stretched into rods using a previously described film stretching method (*26*). Briefly, 100 μl of the original particle stock was added to 10 ml of 7% PVA and dried to a film via overnight incubation at 45°C in a single-well Omni Tray. After 24 hours, the dried film was peeled off the tray and cut into 3 × 1–cm pieces and stretched at 200°C using a syringe pump. The AR of the particles was adjusted by changing the total draw volume of the pump. The films were first washed by dissolving them in 70% isopropanol solution and then subsequently with water to remove the residual PVA. The particles were characterized via SEM imaging using a JEOL JSM-7800FLV SEM microscope. The suspension of the particles was dried on a glass stub and sputter coated with gold before the imaging. The size of the particles was measured using ImageJ software. The size is reported as the average of at least 50 measurements from multiple images. For zeta potential measurements, particles were resuspended in deionized water (5×10^7 particles/ml for microparticles and 5×10^9 particles/ml for nanoparticles), and the zeta potentials were measured using a Malvern ZEN3600 Zetasizer.

Fabrication of the Cy5.5-loaded PLGA rods and spheres

Conjugates of PLGA and Cy5.5 amine dyes were fabricated using EDC/NHS chemistry. Polymer (0.002 mmol) was dissolved in 5 ml of DCM in a 20-ml scintillation vial and mixed with 1.7 mg of EDC in 1 ml of DCM for 5 min. NHS (1.0 mg) in 0.5 ml of DCM was added dropwise to the mixture and allowed to stir for 10 min. Last, 1.5 mg of Cy5.5 amine dye in 1 ml of DCM was added to the mixture and stirred overnight. The solution was purified using 3500–molecular weight cutoff dialysis membrane in 4 liters of distilled water over 3 days.

Rod-shaped PLGA particles were fabricated by the modified two-step emulsion solvent evaporation technique previously described (*34*). Briefly, 25 mg of acid-terminated 50:50 PLGA polymer and 0.5 mg of Cy5.5-conjugated PLGA were dissolved in 10 ml of chloroform. The oil phase was slowly injected into 50 ml of the water phase containing 1% PVA and 3% SMP at pH 8.4 while being continuously stirred at 5500 rpm via a Caframo overhead mixer. The emulsion was mixed for 15 min, and then 50 ml of the second step water phase solution containing 5% PVA and 3% SMP at pH 8.4 was added to the mixture to induce a viscosity shock and enable stretching of the droplets to rods. The emulsion was then stirred for an additional 2 hours to allow the complete evaporation of the oil phase and then centrifuged at 5500 rpm for 15 min to collect the particles and washed twice with water afterward. The spherical particles of the same volume were fabricated via the same protocol and replacing SMP in the water phases with 0.2% Trizma base. The particles were subsequently freeze dried using a Labconco lyophilizer and stored at −20°C until usage.

Cell cultures

Rat alveolar macrophages (ATCC CRL2192) were bought from the American Type Culture Collection (ATCC). Upon arrival, the frozen cell vial was thawed and resuspended in 9.0 ml of macrophage culture media (85% Ham's F-12K medium with 2 mM L-glutamine adjusted to contain 1.5 g/liter sodium bicarbonate, ATCC 30-2004) containing 15% heat-inactivated FBS and centrifuged at 125*g* for 7 min. The supernatant was aspirated, and the cells were resuspended in 15 ml of fresh warm media and transferred to a T75 culture flask and incubated at 37°C and 5% CO_2. The concentration of the cells was counted each day, and when the concentration of the floating cells reached 5×10^5 cells/ml, the cells were collected via trypsinization and utilization of a cell scraper. The cell suspension was then centrifuged at 125*g* for 7 min, reconstituted in fresh media to a concentration of 2×10^5 cells/ml, and transferred to a new flask. The cell media were changed two times per week.

Human THP-1 monocytes were purchased from ATCC (ATCC TIB-202). The frozen cells were thawed and added to 10 ml of warm THP-1 media (ATCC formulated RPMI-1640 media with 10% FBS and 0.05 mM mercaptoethanol). The cell suspension was then centrifuged at 200*g* for 7 min to collect the cells. The media were aspirated, and the cells were resuspended in 10 ml of fresh media and transferred to a T75 flask and incubated at 37°C and 5% CO_2. When the concentration of the cells reached 10^6 cells/ml, the cells were centrifuged, diluted to a concentration of 2×10^5 cells/ml, and transferred to new flasks. The media were refreshed three times per week.

Isolation of the bone marrow–derived macrophages and dendritic cells

Macrophages and dendritic cells were generated as previously described (*42*). Bone marrow cells were collected by flushing femurs and tibias of mice. The cells were cultured in RPMI 1640 GlutaMAX supplemented with 10% FBS and 1% penicillin-streptomycin. To obtain macrophages, culturing media were further supplemented

with either 20% L929 conditioned media, and macrophages were removed using Cell Dissociation Buffer Enzyme-Free Hanks'-Based. To obtain dendritic cells, culture media were supplemented with 50 mM 2-mercaptoethanol and GM-CSF (20 ng/ml), and dendritic cells were obtained from suspension.

In vitro uptake studies

Uptake studies were performed with the general protocol previously described (*20*). For polystyrene whole-blood uptake studies, particles were added to 100 μl of human or mouse blood (at a concentration of 10^7 particles/ml unless specified) and incubated at 37°C and 5% CO_2 for 2 hours. Competitive uptake studies were performed by incubating the same concentration (5×10^6 particles/ml) of the 2-μm carboxylate polystyrene sky blue spheres and green rods of the same volume in whole blood for 2 hours. For PLGA particles, the particle concentration was set at 5×10^7 particles/ml, and the uptake time was reduced to 30 min. The samples were then stained with CD45 and CD11b antibodies (human blood) or CD45, CD11b, ly6G, and ly6C antibodies (mouse blood) for 30 min on ice. Afterward, 2 ml of 1× lyse-fix solution was added to each sample to lyse the red cells and fix the white blood cells and incubated with the samples for 1 hour at room temperature. The samples were then centrifuged at 500*g* for 5 min and washed with fluorescence-activated cell sorting (FACS) buffer (1× PBS + 2% FBS) three times. The percentage of the particle-positive cells in each sample was quantified via flow cytometry. For imaging the competitive uptake assays, 2-μm spheres and AR6 rods of the same concentration (10^7 particles/ml) were added to the same sample, and the uptake assays were done as previously described. The cells were stained with phycoerythrin (PE) anti-human CD45 antibody, and the particles within the cells were visualized via an inverted Nikon fluorescence microscope.

Human plasma was obtained by centrifuging whole blood at 2250*g* for 20 min. Human monocytes were isolated from whole blood using a human monocyte isolation kit and reconstituted in plasma to a concentration of 10^7 cells/ml and used for uptake studies with the protocol described below.

For macrophages, THP-1 monocytes, and dendritic cells, the cells were reconstituted in RPMI 1640 media at a concentration of 10^7 cells/ml for bone marrow–derived macrophages and 5×10^6 cells/ml for THP-1 monocytes, rat alveolar macrophages, and dendritic cells. One hundred microliters of the cell suspensions was added to each well of a 96-well plate and incubated with particles (10^7 particles/ml unless specified) for 2 hours. For macrophages, the cells were incubated in the plates for 30 min before adding the particles to allow their adherence to the plate. After 2 hours, the macrophages and dendritic cells were detached respectively with trypsin or 1× versene solution. The cells were removed from the wells and transferred to 5-ml Falcon tubes. The samples were then fixed using 2 ml of 4% paraformaldehyde solution for 1 hour. Afterward, the samples were washed three times using FACS buffer at 500*g* for 5 min and run on a flow cytometer to check their association with particles.

Mouse immunization

Female SJL/J mice were purchased from Envigo. Peptide-induced EAE was induced in SJL/J mice as previously reported (*43*). Eight- to 10-week-old female mice were immunized subcutaneously at three spots on the flank with 100 μl of an emulsion of PLP peptide in complete Freund's adjuvant (CFA) containing 200 μg of *M. tuberculosis* H37Ra. Peripheral blood was collected from EAE mice 9 days after immunization.

In vivo uptake studies

Six- to 8-week-old male BALB/c mice were used in the in vivo assays. For the in vivo uptake studies, 1.5×10^9 particles were resuspended in 100 μl of PBS and injected a using tail vein catheter. Thirty minutes after injection, the animals were euthanized, and their blood was drawn into heparin-containing syringes using cardiac punctures. The blood samples were then stained using anti-mouse CD45, anti-mouse/human CD11b, anti-mouse Ly-6G, and anti-mouse Ly-6C for 30 min on ice. Afterward, the samples were lyse fixed and centrifuged at 500*g* for 5 min. The pellet was collected and subsequently washed twice with FACS buffer and ran on a flow cytometer to quantify the uptake of the particles by neutrophils and monocytes. Each condition was repeated for five individual animals.

In vivo biodistribution studies

Male BALB/c mice (6 to 8 weeks old) were used in the biodistribution studies. Briefly, 100 μl of 500-nm sky blue polystyrene spheres or AR6 rods of the same volume in PBS was intravenously injected using a tail vein catheter (1.5×10^9 particles/ml). Thirty minutes after injection, the animals were euthanized, and different organs were removed. The animal blood was collected via cardiac puncture. Whole-organ scans were performed via an Odyssey CLx Infrared Imaging System (LI-COR) using the 700-nm channel. Total fluorescence in each organ was quantified using Image Studio Software. Untreated organs were used as a background, and their signal was subtracted from the signal of each organ. The fluorescence signal in all organs of each animal was quantified, and the percentage of injected dosage (ID%) in each organ was quantified via dividing its signal by the total fluorescence signal. The individual organs were weighed, and the data were reported as the %ID per gram of each of the organs.

Statistical analysis

Statistical analysis of the data was performed using GraphPad Prism. Each data point was replicated for at least $n = 3$. Depending on the sets of the data, unpaired *t* test, one-way analysis of variance (ANOVA) with Tukey's posttest (95% confidence interval), or two-way ANOVA with Bonferroni posttests were used to compare the significance of different points.

SUPPLEMENTARY MATERIALS

Supplementary material for this article is available at http://advances.sciencemag.org/cgi/content/full/6/24/eaba1474/DC1

View/request a protocol for this paper from *Bio-protocol*.

REFERENCES AND NOTES

1. D. C. Dale, L. Boxer, W. C. Liles, The phagocytes: Neutrophils and monocytes. *Blood* **112**, 935–946 (2008).
2. C. H. Wu, C. H. Hsieh, S. H. Huang, J. W. Lin, T. D. Wang, S. C. Hsu, Y. M. Wu, T. M. Liu, *In vivo* imaging flow cytometry of human leukocytes. *Opt Life Sci.* BoW3A-2 (2017).
3. G. K. Aulakh, Neutrophils in the lung: "The first responders". *Cell Tissue Res.* **371**, 577–588 (2017).
4. E. Saito, R. Kuo, R. M. Pearson, N. Gohel, B. Cheung, N. J. C. King, S. D. Miller, L. D. Shea, Designing drug-free biodegradable nanoparticles to modulate inflammatory monocytes and neutrophils for ameliorating inflammation. *J. Control. Release* **300**, 185–196 (2019).
5. S. W. Jones, R. A. Roberts, G. R. Robbins, J. L. Perry, M. P. Kai, K. Chen, T. Bo, M. E. Napier, J. P. Y. Ting, J. M. DeSimone, J. E. Bear, Nanoparticle clearance is governed by Th1 / Th2 immunity and strain background. *J. Clin. Invest.* **123**, 3061–3073 (2013).
6. C. A. Fromen, W. J. Kelley, M. B. Fish, R. Adili, M. J. Hoenerhoff, M. Holinstat, O. Eniola-Adefeso, Neutrophil – particle interactions in blood circulation drive particle clearance and alter neutrophil responses in acute inflammation. *ACS Nano* **11**, 10797–10807 (2017).

7. A. N. Rao, N. M. Kazzaz, J. S. Knight, Do neutrophil extracellular traps contribute to the heightened risk of thrombosis in inflammatory diseases? *World J. Cardiol.* **7**, 829–842 (2015).
8. F. Sônego, J. C. Alves-filho, F. Q. Cunha, Targeting neutrophils in sepsis. *Expert Rev. Clin. Immunol.* **10**, 1019–1028 (2014).
9. G. C. Jickling, D. Liu, B. P. Ander, B. Stamova, X. Zhan, F. R. Sharp, Targeting neutrophils in ischemic stroke: Translational insights from experimental studies. *J. Cereb. Blood Flow Metab.* **35**, 888–901 (2015).
10. K. M. Beeh, J. Beier, Handle with care: Targeting neutrophils in chronic obstructive pulmonary disease and severe asthma? *Clin. Exp. Allergy* **36**, 142–157 (2006).
11. D. R. Getts, R. L. Terry, M. T. Getts, C. Deffrasnes, M. Muller, C. van Vreden, T. M. Ashhurst, B. Chami, D. McCarthy, H. Wu, J. Ma, A. Martin, L. D. Shae, P. Witting, G. S. Kansas, J. Kühn, W. Hafezi, I. L. Campbell, D. Reilly, J. Say, L. Brown, M. Y. White, S. J. Cordwell, S. J. Chadban, E. B. Thorp, S. Bao, S. D. Miller, N. J. C. King, Therapeutic inflammatory monocyte modulation using immune-modifying microparticles. *Sci. Transl. Med.* **6**, 219ra7 (2014).
12. F. Leuschner, P. Dutta, R. Gorbatov, T. I. Novobrantseva, J. S. Donahoe, G. Courties, K. M. Lee, J. I. Kim, J. F. Markmann, B. Marinelli, P. Panizzi, W. W. Lee, Y. Iwamoto, S. Milstein, H. Epstein-Barash, W. Cantley, J. Wong, V. Cortez-Retamozo, A. Newton, K. Love, P. Libby, M. J. Pittet, F. K. Swirski, V. Koteliansky, R. Langer, R. Weissleder, D. G. Anderson, M. Nahrendorf, Therapeutic siRNA silencing in inflammatory monocytes in mice. *Nat. Biotechnol.* **29**, 1005–1010 (2011).
13. Y. S. Kang, J. J. Cha, Y. Y. Hyun, D. R. Cha, Novel C-C chemokine receptor 2 antagonists in metabolic disease: A review of recent developments. *Expert Opin. Investig. Drugs* **20**, 745–756 (2011).
14. J. Couzin-Frankel, Roche Exits RNAi Field, Cuts 4800 Jobs. *Science* **330**, 1163 (2010).
15. S. J. Jeong, J. G. Cooper, I. Ifergan, T. L. Mcguire, D. Xu, Z. Hunter, S. Sharma, D. McCarthy, S. D. Miller, J. A. Kessler, Neurobiology of Disease Intravenous immune-modifying nanoparticles as a therapy for spinal cord injury in mice. *Neurobiol. Dis.* **108**, 73–82 (2017).
16. L. M. Casey, S. Kakade, J. T. Decker, J. A. Rose, K. Deans, L. D. Shea, R. M. Pearson, Biomaterials Cargo-less nanoparticles program innate immune cell responses to toll-like receptor activation. *Biomaterials* **218**, 119333 (2019).
17. J. Park, Y. Zhang, E. Saito, S. J. Gurczynski, B. B. Moore, B. J. Cummings, A. J. Anderson, L. D. Shea, Intravascular innate immune cells reprogrammed via intravenous nanoparticles to promote functional recovery after spinal cord injury. *Proc. Natl. Acad. Sci. U.S.A.* **116**, 14947–14954 (2019).
18. T. P. Stossel, B. M. Babior, Structure function and functional disorders of the phagocyte system. in *Blood: Principle and Practice of Hematology*, R. I. Handin, S. E. Lux, T. P. Stossel, Eds. (Lippincott Williams & Wilkins, 2003), pp. 531–568.
19. D. C. Dale, L. Boxer, W. C. Liles, The phagocytes: neutrophils and monocytes. *Blood.* **112**, 935–945 (2008).
20. W. J. Kelley, C. A. Fromen, G. Lopez-cazares, O. Eniola-adefeso, PEGylation of model drug carriers enhances phagocytosis by primary human neutrophils. *Acta Biomater.* **79**, 283–293 (2019).
21. I. García, A. Sánchez-Iglesias, M. Henriksen-Lacey, M. Grzelczak, S. Panades, L. M. Liz-Marzan, Glycans as biofunctional ligands for gold nanorods: Stability and targeting in protein-rich media. *J. Am. Chem. Soc.* **137**, 3686–3692 (2015).
22. C.-M. J. Hu, L. Zhang, S. Aryal, C. Cheung, R. H. Fang, L. Zhang, Erythrocyte membrane-camouflaged polymeric nanoparticles as a biomimetic delivery platform. *Proc. Natl. Acad. Sci. U.S.A.* **108**, 10980–10985 (2011).
23. P. W. Bisso, S. Gaglione, P. P. G. Guimarães, M. J. Mitchell, R. Langer, Nanomaterial interactions with human neutrophils. *ACS Biomater Sci. Eng.* **4**, 4255–4265 (2018).
24. J. A. Champion, A. Walker, S. Mitragotri, Role of particle size in phagocytosis of polymeric microspheres. *Pharm. Res.* **25**, 1815–1821 (2008).
25. M. B. Fish, A. J. Thompson, C. A. Fromen, O. Eniola-adefeso, Emergence and utility of nonspherical particles in biomedicine. *Ind. Eng. Chem. Res.* **54**, 4043–4059 (2015).
26. J. A. Champion, S. Mitragotri, Role of target geometry in phagocytosis. *Proc. Natl. Acad. Sci. U.S.A.* **103**, 4930–4934 (2006).
27. J. A. Champion, S. Mitragotri, Shape induced inhibition of phagocytosis of polymer particles. *Pharm. Res.* **26**, 244–249 (2009).
28. G. Sharma, D. T. Valenta, Y. Altman, S. Harvey, H. Xie, S. Mitragotri, J. W. Smith, Polymer particle shape independently influences binding and internalization by macrophages. *J. Control. Release* **147**, 408–412 (2010).
29. D. M. Richards, R. G. Endres, How cells engulf: A review of theoretical approaches to phagocytosis. *Rep.Prog. Phys.* **80**, 126601 (2017).
30. J.-W. Yoo, E. Chambers, S. Mitragotri, Factors that control the circulation time of nanoparticles in blood: Challenges, solutions and future prospects. *Curr. Pharm. Des.* **16**, 2298–2307 (2010).
31. A. J. Thompson, E. M. Mastria, O. Eniola-adefeso, The margination propensity of ellipsoidal micro / nanoparticles to the endothelium in human blood flow. *Biomaterials* **34**, 5863–5871 (2013).
32. S. Honary, F. Zahir, Effect of zeta potential on the properties of nano-drug delivery systems- A review (Part 2). *Trop. J. Pharm. Res.* **12**, 265–273 (2013).
33. Y. Tabata, Y. Ikada, Effect of the size and surface charge of polymer microspheres on their phagocytosis by macrophages. *Biomaterials* **9**, 352–362 (1988).
34. H. Safari, R. Adili, M. Holinstat, O. Eniola-Adefeso, Modified two-step emulsion solvent evaporation technique for fabricating biodegradable rod-shaped particles in the submicron size range. *J. Colloid Interface Sci.* **518**, 174–183 (2018).
35. X. Huang, L. Li, T. Liu, N. Hao, H. Liu, D. Chen, F. Tang, The shape effect of mesoporous silica nanoparticles on biodistribution, clearance, and biocompatibility *in vivo*. *ACS Nano* **5**, 5390–5399 (2011).
36. K. Namdee, A. J. Thompson, A. Golinski, S. Mocherla, D. Bouis, O. Eniola-Adefeso, *In vivo* evaluation of vascular-targeted spheroidal microparticles for imaging and drug delivery applications in atherosclerosis. *Atherosclerosis* **237**, 279–286 (2014).
37. C. K. Huang, Protein Kinases in Neutrophils: A Review. *Membr. Biochem.* **8**, 61–79 (1989).
38. M. Herant, C. Lee, M. Dembo, V. Heinrich, Protrusive push versus enveloping embrace: Computational model of phagocytosis predicts key regulatory role of cytoskeletal membrane anchors. *PLOS Comput. Biol.* **7**, e1001068 (2011).
39. V. Heinrich, Biophysical perspective controlled one-on-one encounters between immune cells and microbes reveal mechanisms of phagocytosis. *Biophys. J.* **109**, 469–476 (2015).
40. R. C. May, L. M. Machesky, Phagocytosis and the actin cytoskeleton. *J. Cell Sci.* **114**, 1061–1077 (2001).
41. S. Satish, M. Tharmavaram, D. Rawtani, Halloysite nanotubes as a nature's boon for biomedical applications. *Nanobiomedicine* **6**, 1–16 (2019).
42. R. Kuo, E. Saito, S. D. Miller, L. D. Shea, Peptide-conjugated nanoparticles reduce positive co-stimulatory expression and T cell activity to induce tolerance. *Mol. Ther.* **25**, 1676–1685 (2017).
43. S. D. Miller, W. J. Karpus, T. S. Davidson, Experimental autoimmune encephalomyelitis in the mouse. *Curr. Protoc. Immunol.* **88**, 15.1.1–15.1.20 (2010).

Acknowledgments: We thank A. Banka, G. Lopez-Cazares, and M. Gutierrez for technical Assistance. **Funding:** This work was supported by the University of Michigan Barbour Scholarship to H.S., Falk Medical Research Trust (AWD013948) and Mi-Kickstart grant to O.E.-A., and NIH R01 (EB013198) to L.D.S. E.S. was supported by R01EB013198. **Author contributions:** H.S. and O.E.-A. wrote the paper. All the authors contributed in designing and performing the experiments and revising the manuscript. **Competing interests:** L.D.S. serves as a consultant for Cour Pharmaceuticals. The authors declare that they have no other competing interests. **Data and materials availability:** All data needed to evaluate the conclusions in the paper are present in the paper and/or the Supplementary Materials. Additional data related to this paper may be requested from the authors.

Submitted 8 November 2019
Accepted 14 April 2020
Published 10 June 2020
10.1126/sciadv.aba1474

Citation: H. Safari, W. J. Kelley, E. Saito, N. Kaczorowski, L. Carethers, L. D. Shea, O. Eniola-Adefeso, Neutrophils preferentially phagocytose elongated particles—An opportunity for selective targeting in acute inflammatory diseases. *Sci. Adv.* **6**, eaba1474 (2020).